Polymer 49 (2008) 4248–4258

Contents lists available at ScienceDirect

Polymer

journal homepage: www.elsevier.com/locate/polymer

Morphology and properties of thermoplastic polyurethanes with dangling chains in ricinoleate-based soft segments

Yijin Xu [a,*], Zoran Petrovic [a], Sudipto Das [b], Garth L. Wilkes [b]

[a] Kansas Polymer Research Center, Pittsburg State University, Pittsburg, KS 66762, United States
[b] Department of Chemical Engineering, Virginia Polytechnic Institute and State University, Blacksburg, VA 24061, United States

ARTICLE INFO

Article history:
Received 18 June 2008
Received in revised form 11 July 2008
Accepted 14 July 2008
Available online 24 July 2008

Keywords:
Biopolymers
Segmented polyurethanes
Dangling chain

ABSTRACT

In our previous publication on the structure–property behavior of segmented polyurethanes based on castor oil [Petrović ZS, Xu Y, Zhang W. Polymer Preprints 2007;48(2):852–3.], the results showed that these materials which possessed a soft segment weight concentration (SSC) of 70% have both low tensile strength and elongation at break. This behavior is distinctly different from segmented polyurethanes of comparable soft segment content obtained from petrochemical polymeric diols that possess terminal hydroxyl groups. The poor elastic properties of these segmented polyurethanes were ascribed to the low molecular weight of the polymers as well as due to the presence of the six-carbon "dangling chain", which may influence the morphology of the resulting segmented polyurethanes. To further understand this behavior, four segmented polyurethanes with the SSC of 70, 60, 50, and 40%, respectively, were synthesized from a polyricinoleate diol with an M_n of 2580, diphenylmethane diisocyanate (MDI) and butanediol. The objective of this work was to study the effect of SSC on the morphology of the resulting polyurethanes, and to correlate the morphology with the properties of these bio-based segmented polyurethanes. Polymers were characterized by GPC, viscometry and spectroscopic methods. Thermal and mechanical properties of the polymers indicated good microphase separation. Microphase morphology was also noted by SAXS and AFM. Finally, "spherulitic-like" superstructures were noted in the solution cast films that are believed to arise from the nucleation and crystallization of the hard segments.

1. Introduction

Segmented polyurethane elastomers are block copolymers with alternating soft and hard blocks that, due to structural differences/incompatibility, separate into microphases or domains formed from the respective hard and soft segments. Hard domains play the role of physical crosslinks and act as a high modulus filler, whereas the soft phase provides extensibility [2–5]. The morphology of segmented PUs depends on the structure and relative amount of these soft and hard phases and their ordering. Soft segments in the work discussed in this paper were made from ricinoleic acid which is the major component of castor oil, while the hard segments are of petrochemical origin. Polyurethanes with a 70 wt% soft segment concentration (SSC) typically have non-spherical hard domains dispersed in the matrix of soft segments, while co-continuous phase morphologies have been postulated in the samples with 50 wt% SSC [6,7]. Reports also exist in the literature that demonstrate that if the hard segments can undergo crystallization, it may be possible to even develop spherulitic superstructures in such segmented systems [8–12]. In general, polyurethanes with 70% SSC are soft thermoplastic rubbers whereas those with 50% SSC are more commonly viewed as hard rubbers, both being of significant industrial importance.

The utilization of natural products such as plant oils and natural fats has attracted great attention in both scientific and industrial areas in recent years, due to both the energy and the environmental considerations. These starting materials are sustainable, renewable, and most importantly, biodegradable. The general chemical composition of plant oils and natural fats is triacylglycerols, of which the fatty acids are in majority composed of oleic acid, linoleic acid, and linolenic acid; and in minority comprise saturated fatty acids with the chain length from C_6 to C_{18}. By modifications of the ester groups and double bonds, a broad spectrum of polymeric materials has been made and some of them have played a significant role in our daily lives already [13–22]. Most of the polymer materials made from these bio-based feedstocks are, however, cross-linked materials (thermoset) except for a very few reports on syntheses of thermoplastics using either metathesis or an ozonolysis pathway, which means some parts of the original triacylglycerol were not utilized [20,23]. A major application of the

* Corresponding author. Tel.: +1 620 235 6594.
E-mail address: yxu@pittstate.edu (Y. Xu).

0032-3861/$ – see front matter © 2008 Elsevier Ltd. All rights reserved.
doi:10.1016/j.polymer.2008.07.027

feedstocks derived from the plant oils and natural fats is in the polyurethane industry [24], but again, at this time, these polyurethanes are all chemically cross-linked [25–29]. Good properties and wide applications of thermoplastic polyurethanes, combined with the potential biocompatibility and biodegradability of bio-based feedstocks, stimulated us to synthesize segmented polyurethanes from vegetable oils that could be melt processable. Specifically, thermoplastic polyurethanes (TPUs) made from vegetable oils are processed by injection molding and extrusion and as such would be suitable for sporting goods and other products of limited lifetime. To the best of our knowledge, the following report is the first to address this approach. Elastomers of somewhat similar structures based on polyricinoleic acid were suggested as internal release agents [30].

In order to synthesize the polyester diols for the preparation of thermoplastic polyurethanes, mono-hydroxylated fatty acids (or their esters) have to be first derived from natural oils by epoxidation followed by hydroxylation, or from castor oil by hydrolysis or methanolysis; then the mono-hydroxylated fatty acids or esters may be polymerized into polyester diols through condensation polymerization [1,31]. Here we choose ricinoleic acid from castor oil as a model hydroxylated fatty acid because it has a well-defined structure: an 18-carbon fatty acid with a hydroxyl group on the 12th carbon and *cis*-double bond between C_9 and C_{10}. In a previous report [1] we showed that for all the segmented polyurethanes having different polyricinoleate molecular weights, their tensile strength and elongation at break were low at the soft segment concentration (SSC) of 70%, and below those of segmented polyurethanes with comparable soft segment content prepared from petrochemical resources. Properties of segmented polyurethanes based on polyricinoleic acid soft segments depend not only on the structure of the soft segments but also on the soft segment length and concentration as well as on the final morphology developed. Dangling chains in the soft segment appear to have a strong effect on the morphology and thus properties of these TPUs. The objective of this work was to obtain a better understanding of the effect of structure on morphology and properties. We synthesized a series of polyurethanes with the fixed soft segment molecular weight of 2580 and varied SSCs (70, 60, 50 and 40%). Here we report their physical, thermal and mechanical properties together with some additional information on their morphologies.

2. Experimental

2.1. Materials

Mondur M from Bayer is a pure diphenylmethane diisocyanate (MDI) with a melting temperature of 40 °C and isocyanate content of 33.5%. It was purified by vacuum distillation and used within 7 days for the synthesis of polyurethanes. 1,4-Butanediol was purchased from Aldrich, purified by vacuum distillation and stored on molecular sieves. Anhydrous *N*,*N*′-dimethyl acetamide (DMAC) and HPLC grade *N*,*N*′-dimethyl formamide (DMF) were bought from Sigma–Aldrich and used as-received.

Methyl ricinoleate (MR) was obtained from castor oil by conventional methanolysis. The crude methyl ricinoleate was purified by multiple vacuum distillations. Both GPC and DSC results confirmed that its purity was higher than 99%.

Polyricinoleate diols were synthesized via polycondensation (transesterification) of highly purified methyl ricinoleate (OH# = 180 mg KOH/g) with diethylene glycol (DEG) as initiator as follows: into a 500 mL round-bottomed flask were charged 112.4 g of methyl ricinoleate (0.36 mol), 6.67 g of diethylene glycol (0.063 mol), and 0.585 g of FasCat® 4325. The mixture was heated at 190–200 °C under nitrogen flushing, methanol came out immediately. Medium vacuum was applied after 105 min: 1 h at 170–180 °C followed by another hour at 200–210 °C. The reaction content was finally heated at 180–200 °C for 30 min. All the distillate during vacuum process was collected for GPC analysis. After the reaction content was cooled down to room temperature, 300 mL of diethyl ether was added for dilution and 1.5 g of carbon black was added for de-coloring, and the mixture was stirred overnight at room temperature. After carbon black was filtered off, the filtrate was washed with distilled water. Solvent was removed under vacuum and the product was finally dried at 85 °C under high vacuum for about 1 h. The properties of the diol used in the synthesis of segmented polyurethanes are listed in Table 1. Fig. 1 depicts the structure of the polyricinoleate diol.

2.2. Synthesis of segmented polyurethanes

Thermoplastic polyurethanes were synthesized by a one-pot two-step polymerization process. Fig. 2 illustrates the synthetic pathway. A typical reaction is as follows: the prescribed amount of polyricinoleate diol, which was pre-dried under vacuum at 75–80 °C for about 1.5 h, was then transferred into a 100 mL three-necked round-bottomed flask which was equipped with a magnetic stirrer bar, a vacuum outlet, a dry nitrogen inlet, and a reflux condenser. Under nitrogen protection, the predetermined amount of MDI was added into the flask. The temperature was kept at 80 °C and the reaction was allowed to proceed for 3 h, after which anhydrous DMAC was added into the prepolymer at the amount to make up about 30 wt% of the final solution. When the prescribed amount of 1,4-butanediol was added into the reaction mixture with a syringe, the temperature was further increased to 90 °C, the polymerization continued overnight. The polyurethanes were purified by precipitating into water. The precipitated granules were separated by filtration and thoroughly washed with water, followed by vacuum drying to constant weight. Polyurethanes with SSCs of 70, 60, 50, and 40% were prepared by this procedure.

2.3. Preparation of cast films for mechanical and thermal characterization

All the TPU films were prepared by solution casting in order to try and promote good microphase separation. A 100 mL round-bottom flask equipped with magnetic stirrer bar was charged with 12 g of TPU and 28 g of DMF (to obtain a 30 wt% solution). The flask was heated on an oil bath at 85 °C. The solution was cast onto a piece of freshly cleaned glass (10 cm × 10 cm) which was pre-heated in a force-draft oven at 65 °C. The oven temperature was decreased to 40 °C after 4 h, and kept at this temperature for another 6 h, after which the film coated glass plate was taken out and cooled to room temperature. After peeling the film from the glass plate, any residual solvent in the film was further removed in a vacuum oven to constant weight. The film was kept in a desiccator for future characterization. A thin film was also cast on a KBr plate at the same time for FTIR characterization.

2.4. Characterization methods

The hydroxyl value of the polyol was determined according to the ASTM E 1899-97 test method using a reaction with

Table 1
Designation and properties of methyl ricinoleate and polyricinoleate diol

Designation	OH#, mg KOH/g	M_n (calculated from OH#)	Acid value, mg KOH/g	Viscosity, Pa s
MR	180	306	3.2	0.024
PR diol	43.5	2580	0.68	1.47

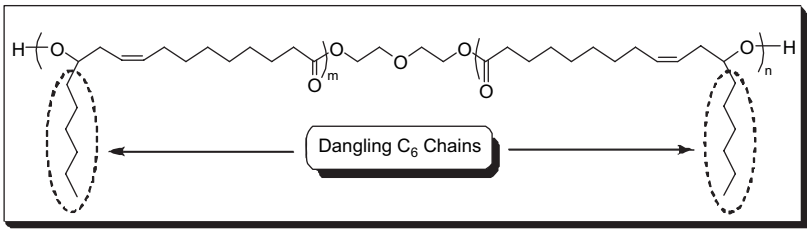

Fig. 1. Structure of polyricinoleate diol prepared by polycondensation.

p-toluenesulfonyl isocyanate (TSI) and potentiometric titration with tetrabutylammonium hydroxide.

Viscosity was measured on an AR 2000 dynamic stress rheometer from TA Instruments, New Castle, DE, USA.

The FTIR spectra were recorded on a Spectrum-1000 Fourier transform infrared (FTIR) spectrometer from Perkin Elmer, Waltham, MA, USA, scanning from 500 to 4000 cm^{-1} at the resolution of 2 cm^{-1} and interval of 0.5 cm^{-1}, 16 scans were collected for each sample.

The GPC chromatograms were obtained on a Waters system consisting of the 510 pump and 410 differential refractometer. Tetrahydrofuran was used as eluent at 1.00 mL/min at 30 °C. Four Phenogel columns (300×7.8 mm ID; particle size is 5 μm; pore sizes are 50, 100, 10^3, and 10^4 Å, respectively) plus a guard Phenogel column from Phenomenex were used; monodisperse polystyrene standards covering a MW range of 10^2–5×10^5 were used for calibration.

DSC thermograms were recorded on a DSC Q100 (TA instruments). The samples were first cooled down to −90 °C and then heated to a temperature above their melting points at the ramping rate of 10 °C/min. A thermal analysis system from TA Instruments, New Castle, DE, USA, consisting of the Controller 3100 with Thermomechanical (TMA) 2940 module, thermogravimetric analyzer (TGA) 2050 module was used to measure the glass transition and thermal stability. The TGA experiments were conducted in a nitrogen atmosphere from room temperature to 600 °C at a heating rate of 20 °C/min.

Dynamic mechanical tests were carried out on DMA 2980 from TA Instruments at 1 Hz and heating rate of 3 °C/min. Tensile properties were measured according to ASTM D882-97 using a tensile tester model 4467 from Instron, Canton, MA, USA.

The free or "air exposed" surface morphology of the polyurethane solution cast films was analyzed by field emission scanning electron microscopy (SEM). The samples were adhered to aluminum sample holders and sputter coated with Au–Pd to a thickness of *ca.* 10 nm. The samples were then inserted in a Leo 1550 FESEM and micrographs were obtained at a working distance of *ca.* 26 mm and accelerating voltage of 20 kV.

The phase images of the polyurethane samples were obtained using a VEECO Dimension 3000 atomic force microscope with Nanoscope IIIA controller. Images were obtained under ambient conditions using Nanodevices TAP150 silicon cantilever probe tips (5 N/m spring constant, ~100 kHz resonant frequency). The samples were fractured under liquid nitrogen manually. Several samples were fractured by the above procedure and a relatively flat surface was elected for AFM characterization. The fractured sample was then brought back to room temperature and mounted on a special sample holder. The phase images of the fractured surfaces were obtained under ambient conditions. During image acquisition, the free air amplitude was normally set at 2.8 V and the set point ratio was in the range of 0.4–0.7, which constitutes hard to medium tapping, respectively.

Pin-hole collimated small angle X-ray scattering (SAXS) profiles were collected for samples under vacuum but at room temperature using a Bruker AXS instrument.

3. Results and discussion

3.1. Structure of polyricinoleate diol and segmented polyurethanes

FTIR spectrum of methyl ricinoleate shows a broad hydroxyl peak between 3650 and 3100 cm^{-1}, double bond at 3007 cm^{-1} and

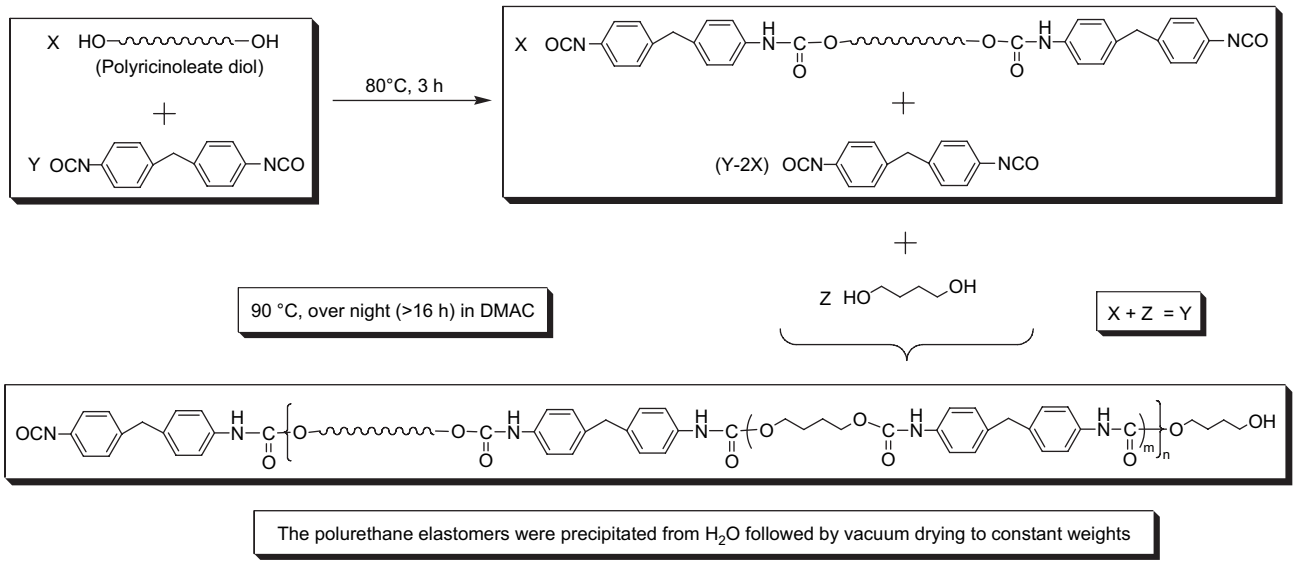

Fig. 2. Illustration for the synthesis of polyurethanes.

a characteristic triglyceride ester carbonyl at 1741 cm^{-1}. At low concentration of hydroxyls as in polyricinoleate diol, hydroxyl peak in the very hydrophobic environment is split into two bands at 3536 and 3455 cm^{-1}, the former being assigned to the non-hydrogen bonded and the latter to hydrogen-bonded hydroxyls. The chemical composition of the segmented polyurethanes based on polyricinoleate soft segment is characterized by free ester carbonyls at 1733 cm^{-1}, double bonds at 3011 cm^{-1} and ester –C–O vibration in the region of 1100–1200 cm^{-1} from the soft segments; and characteristic urethane bands such as free carbonyl at 1733 cm^{-1}, an NH band at about 3336 cm^{-1} and an amide II absorption at 1540–1560 cm^{-1}. Fig. 3 shows the FTIR spectra of MR, polyricinoleate and the four polyurethanes with different SSCs. The N–H bands were observed to move to lower wavenumbers suggesting hydrogen bonding between either the hard segments or between hard segments and soft segments. The peak centered at 1703 cm^{-1} is ascribed to the vibration of hydrogen-bonded carbonyls from both triglyceride ester and urethane groups. With the increase of hard segment concentration, the peak at 1703 cm^{-1} increases as expected, while the peak at 1733 cm^{-1} from the free carbonyl group decreases.

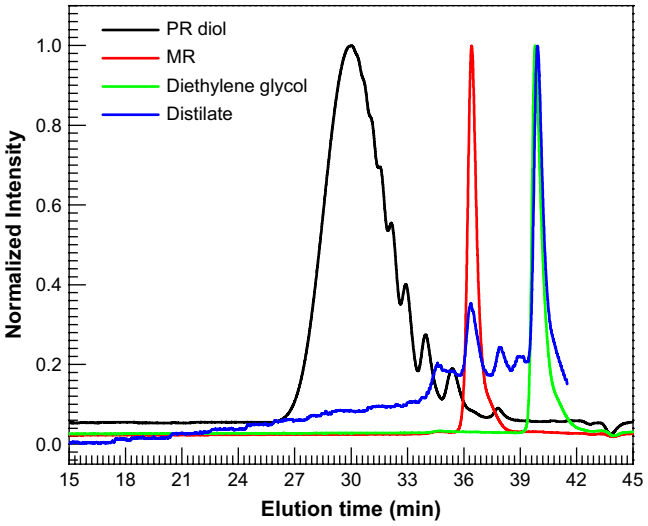

Fig. 4. Overlay of GPC curves for methyl ricinoleate, diethylene glycol, and the polyricinoleate diol prepared from methyl ricinoleate and diethylene glycol.

3.2. Molecular weight distribution of polyricinoleate diol and segmented polyurethanes

Fig. 4 overlays the GPC traces of the polyricinoleate diol together with the starting materials which constituted methyl ricinoleate and diethylene glycol. Polyricinoleate diol shows the molecular weight distribution typical for polycondensation polymers. Low molecular species are observed as separate peaks while higher MW species merge into a single peak. The peak at 35.4 min is believed to arise from the cyclics formed during the polycondensation process, which remains unchanged in the polyurethanes synthesized with this polyricinoleate diol. The TSI method gave an OH# of 43.5 (average of three measurements), from which the number average molecular weight of the polyricinoleate is calculated to be 2580 g/mol, assuming that each polyricinoleate molecule has two hydroxyl groups; the M_n from GPC is 2524 (against narrow distribution polystyrene standards) and PDI (polydispersity) is 1.61. The experimental molecular weight of 2580 (from OH#) is higher than the target molecular weight of 1800 based on the assumption that all the diethylene glycol went into polyricinoleate chains, each polyricinoleate chain has one diethylene glycol chain on average and all the methyl ester groups participated in polycondensation. The higher molecular weight is due to the loss of diethylene glycol and methyl ricinoleate during the vacuum process at high temperatures. More of diethylene glycol was lost than methyl ricinoleate, which can be seen clearly from Fig. 4. Fig. 5 depicts the GPC results for polyurethanes with 70, 60, and 50% SSCs. The segmented polyurethane with 40% SSC did not dissolve well in THF and hence was not characterized by GPC. Results showed that an increase in SSC content led to polyurethanes with lower molecular weights. All samples had a small amount of oligomers in the region around 35 min of elution time. The samples with 50 and 60% SSC displayed a small amount of high molecular weight species in the region of 17 min, which may be due to allophanate formation. Number average molecular weights relative to polystyrene were 23,489 (PDI = 3.32) for PU-50 SSC, 21,510 (PDI = 4.10) for PU-60 SSC, and 14,848 (PDI = 4.68) for PU-70 SSC. Intrinsic viscosities of the samples measured in DMF were below 0.5 dL/g indicating relatively low molecular weights which would likely affect mechanical properties (0.2, 0.24, 0.38, and 0.36 for PU-70, 60, 50, and 40, respectively). Thus, while the optimal mechanical

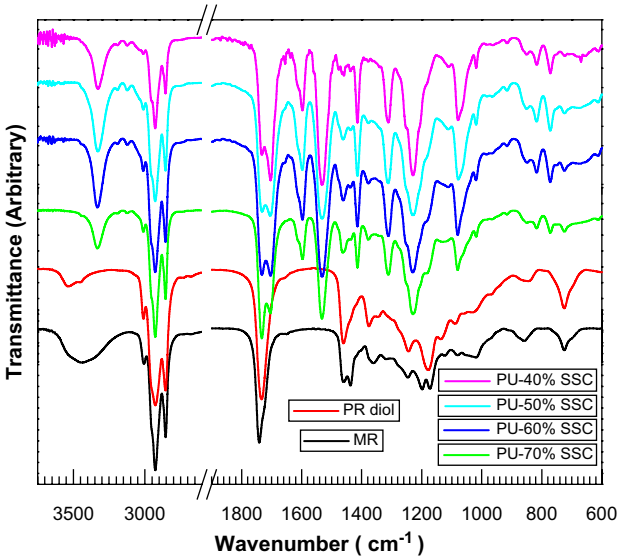

Fig. 3. FTIR comparison for polyricinoleate diol and the four polyurethanes.

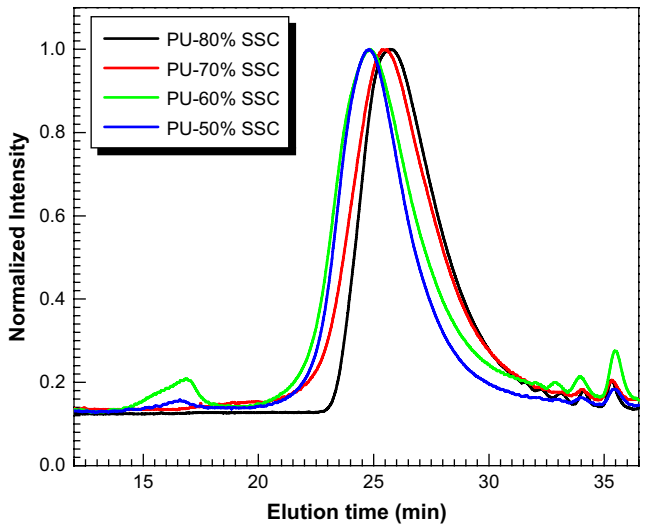

Fig. 5. GPC curves for segmented polyurethanes with 70, 60, and 50% SSC.

properties may not be obtained without reaching higher molecular weights, the general morphology and structure–property relationships as a function of SSC would still hold. One of the issues with this type of polyols is their functionality. The cyclics present in the polyol, which are always formed in condensation reactions, are not detrimental to the polyurethane formation, but even a slight unsaturation as a result of dehydratation which may occur at temperatures around 200 °C would reduce functionality of the diol and thus the molecular weight of the respective polyurethanes. Detecting double bonds formed in the presence of a large number of double bonds from the ricinoleic acid may not be precise enough.

3.3. Morphological investigation of segmented polyurethanes by SEM

As stated earlier, all film materials were prepared by solution casting from DMF as compared to preparation from the melt. While all films, irrelevant of HS content were quite transparent, the upper or "air" surface was investigated by SEM to note if any superstructure texture was observed. Somewhat surprisingly, it was seen that the film materials were found to display a "spherulitic-like" texture. Two examples of this are shown in Fig. 6a and b – which display the film surfaces of the two extreme hard segment contents.

One notes from these micrographs that the general size of these superstructures is on the order of 10 μm with the 60% HS content sample showing slightly larger size superstructures than in the 30% HS sample. While first indications of this structure do suggest that these ball-like structures arise from the nucleation and crystallization of the HS units which could lead to a spherulitic texture, no distinct signs of interconnected crystalline growth could be seen with SEM at the surface even with higher magnification or through the use of AFM (see later discussion below). The lack of crystalline fibrillar growth in these structures might be caused by the non-uniformity of HS lengths in a given sample thereby impairing longer range ordering but this is only a conjecture. However, it is clear that overall global growth should still occur once a given group of HSs nucleate which puts more restrictions on other nearby segments which, in turn, should help promote their nucleation as well. The fact that all films were quite transparent suggests that these structures may not be particularly optically anisotropic as found in conventional spherulitic superstructure commonly observed in crystalline homopolymers. This is not to say that segmented urethanes cannot form such anisotropic bodies for indeed work by the two principal authors have shown that there are cases where very distinct optically anisotropic spherulitic structures can be formed during film preparation [8,9]. However, in these latter cases, the segment chemistries were quite different for the chain structures relative to those utilized in the present report [8–12]. To further substantiate that the ball-like structures that are shown in Fig. 6a and b are not optically anisotropic, the well known technique of small angle light scattering (SALS) was applied to these materials in the same manner as has been used by one of the authors in previous studies where very distinct optically anisotropic spherulitic entities were observed in cast films of monodisperse hard segment based urethanes that utilized PTMO, poly(tetramethylene oxide), as the soft segment [9–11]. It was found in the present study that no sign of any prominent H_v (anisotropic) scattering was observed nor any azimuthal dependence of what little scattering did occur. We also saw no sign of a Maltese cross when any of the superstructures when observed by polarizing optical microscopy (POM). The lack of any azimuthally dependent H_v SALS pattern in conjunction with no Maltese cross or related sign of optical anisotropy using POM further supports why the present films are quite transparent. It is our tentative hypothesis that the origin of these superstructures within the films begin with the nucleation of HS crystalline domains. These further grow with time and gain considerable size. They encompass not only HS domains but also incorporate SS material as well. Due to what is likely poor directional order, there is little to no significant optical anisotropy induced along the radius making them nearly globally isotropic. Further work along this line would be of interest to better test this hypothesis. Finally, we also noted the uniaxial deformation behavior of these superstructures – one example being shown in Fig. 7A and B which provides two different magnification micrographs for the material having the highest HS content. The film had been stretched to about 150% elongation at ambient and then clamped to restrict any recovery. It was then sputter coated and investigated.

Note that the superstructures do elongate and somewhat flatten although their general outline is still maintained – note Fig. 7B. The fact that these structures do impinge but not necessarily in a uniform manner at their boundaries suggests that such non-uniformities may influence the local stress state when deformed and hence particularly the ultimate properties (locus of failure) may also be influenced. We will raise this point again later in this report.

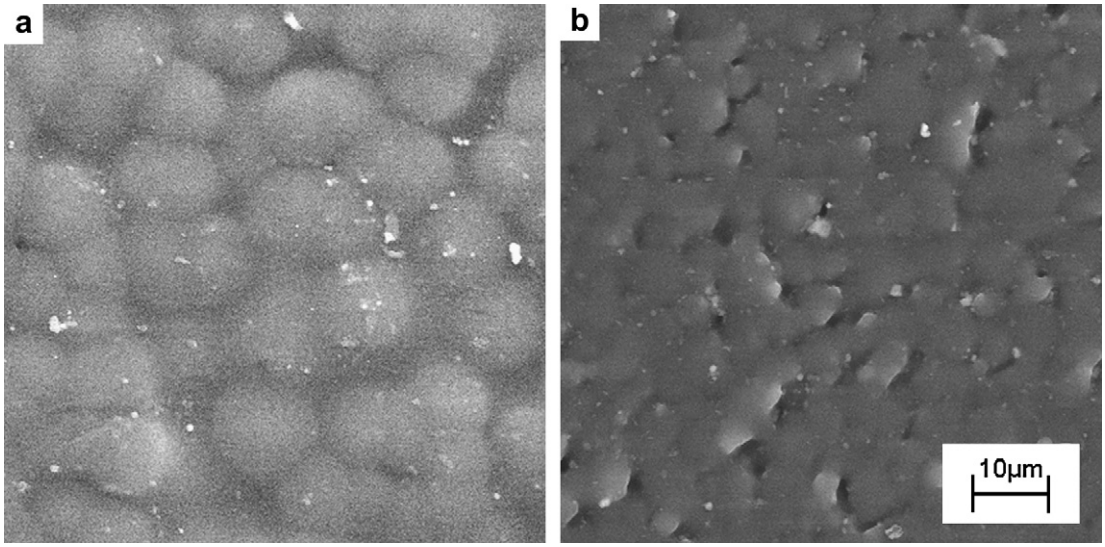

Fig. 6. SEM micrographs of the air surface of undeformed, solution cast polyurethane films with various hard segment contents (a) 60 and (b) 30 wt%.

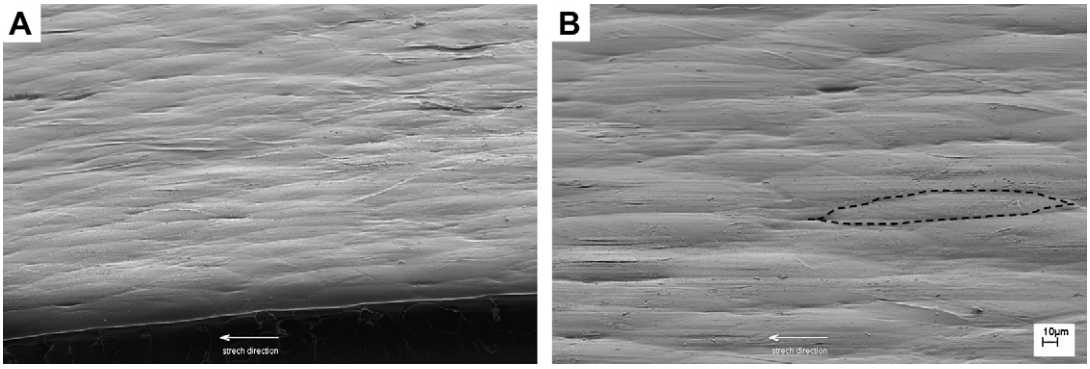

Fig. 7. SEM micrographs of the air surface of a solution cast polyurethane film containing 60 wt% hard segments which has been stretched *ca.* 150%: (A) 1000 (B) 2000 magnification [sample was tilted 57° with respect to the electron beam; horizontal deformation direction].

3.4. Morphological investigation of segmented polyurethanes by AFM

One feature of segmented polyurethanes prepared from polyricinoleate diol is that the cast films with the thickness of 0.5–1 mm were all quite transparent as stated above, which is attributed to a domain size smaller than the wave length of light rather than matching indices of the aliphatic soft and aromatic hard segments. To further confirm the presence of a microphase separated morphology indirectly deduced by DSC and DMA results, we performed tapping mode AFM experiments on the fractured surfaces of the segmented polyurethane samples to try and directly observe if the presence of a microphase morphology existed and how that varied with SS content. The results are shown in Fig. 8.

In Fig. 8a, one notes a near uniform matrix with whitish speckled small regions within – the latter regions we believe arise from the more particulate HS domains that would also possess some crystallinity based on DSC data that will be presented later in this report. Above the SSC of 40%, it becomes more difficult to note a distinct microphase texture since there is now a considerable HSC and this causes difficulty in separating one microphase region from another – one of the authors has faced this same problem in past studies of segmented polymers in that as SSC decreased, the ability to easily denote rich SSC vs. HSC regions became more difficult utilizing AFM methodology [12,32]. The AFM phase images shown in Fig. 8 were, however, also found to become progressively "brighter" with increase in the HSC, indicating a systematic increase in the hardness of the samples as would be expected. It might be mentioned that the AFM investigation again did not reveal any further information at higher magnification regarding the superstructures discussed earlier in that no signs of HS crystal connectivity were apparent. To further substantiate the presence of microphase separation, we therefore turned to the use of SAXS to probe this issue as is next discussed.

3.5. Morphology of segmented polyurethanes by SAXS

In contrast to AFM which is basically a surface characterization technique, SAXS is a bulk characterization technique and has been greatly utilized in providing direct evidence for microphase separation in segmented and block copolymers [33,34]. In Fig. 9 we show the scattering profiles of the four segmented urethane systems.

All the polyurethanes showed the presence of a well-defined first order scattering peak indicating the presence of a microphase separated morphology under ambient conditions. The average interdomain spacings in the polyurethanes were calculated from the position of the interference peak in the respective scattering intensity profiles ($\sim s_{max}^{-1}$) in the sample. As expected, the interdomain spacings were found to decrease systematically from 18.1 to 16.1 nm with an increase in the soft segment content from 40 to 70%. As the hard segment content was increased in the segmented polyurethanes while keeping the soft segment length constant, the center-to-center distance between the hard domains increases as shown by the SAXS results. The width at half height of the scattering profiles was also found to decrease slightly with increase in the HSC. From these data which provide a very distinct peak and not just weak shoulder, it implies that the microphase morphology is quite distinct for these bio-based segmented systems and the associated spacing is on the order of those often found in petroleum based segmented analogues.

3.6. Thermal behavior of segmented polyurethanes

DSC thermograms of segmented polyurethanes are often characterized by three typical transitions: the glass transition of the soft segment; the glass transition of the amorphous portion of hard segments and melting of hard segments if hard segment symmetry exists along with suitable thermal history to allow crystallization to occur. MDI/BDO hard segment glass transitions in polyurethanes with polytetramethylene or polypropylene oxide soft segments usually are not clearly observable as with currently studied polyurethanes, indicating that a significant portion in the latter is amorphous, i.e., crystallization does not proceed to the same extent in the presence of fatty acid-based polyols. This could be interpreted in terms of increased miscibility of the hard and soft phases and perhaps smaller more imperfectly packed hard domains. The highest T_g of the hard segment is observed somewhat below 100 °C in the sample with 60% hard segments (40% SSC).

Multiple endothermic peaks of related MDI containing segmented systems have generally been observed in TPUs but this behavior was dependent on segment concentration, segment length and distribution, and especially on thermal history [35–40]. Fig. 10 shows the DSC thermograms for the four samples at a heating rate of 10 °C/min. While it is not very distinct, the glass transition of the hard segments is in the range of 100 °C; however, the T_g of the soft segments became broader with increasing hard segment concentration.

The glass transition temperature of pure polyricinoleate diol is −76 °C at the heating rate of 10 °C/min when heated from −90 °C, which is close to the T_g value of −74.5 °C of high molecular weight polyricinoleate at the same heating rate as recently reported [41]. The broadening of the glass transition of soft segment could be the result of the partial phase mixing of hard segment into the soft segments, but it may also be influenced by the mobility of soft segment chains restricted by hard domains due to the formation of

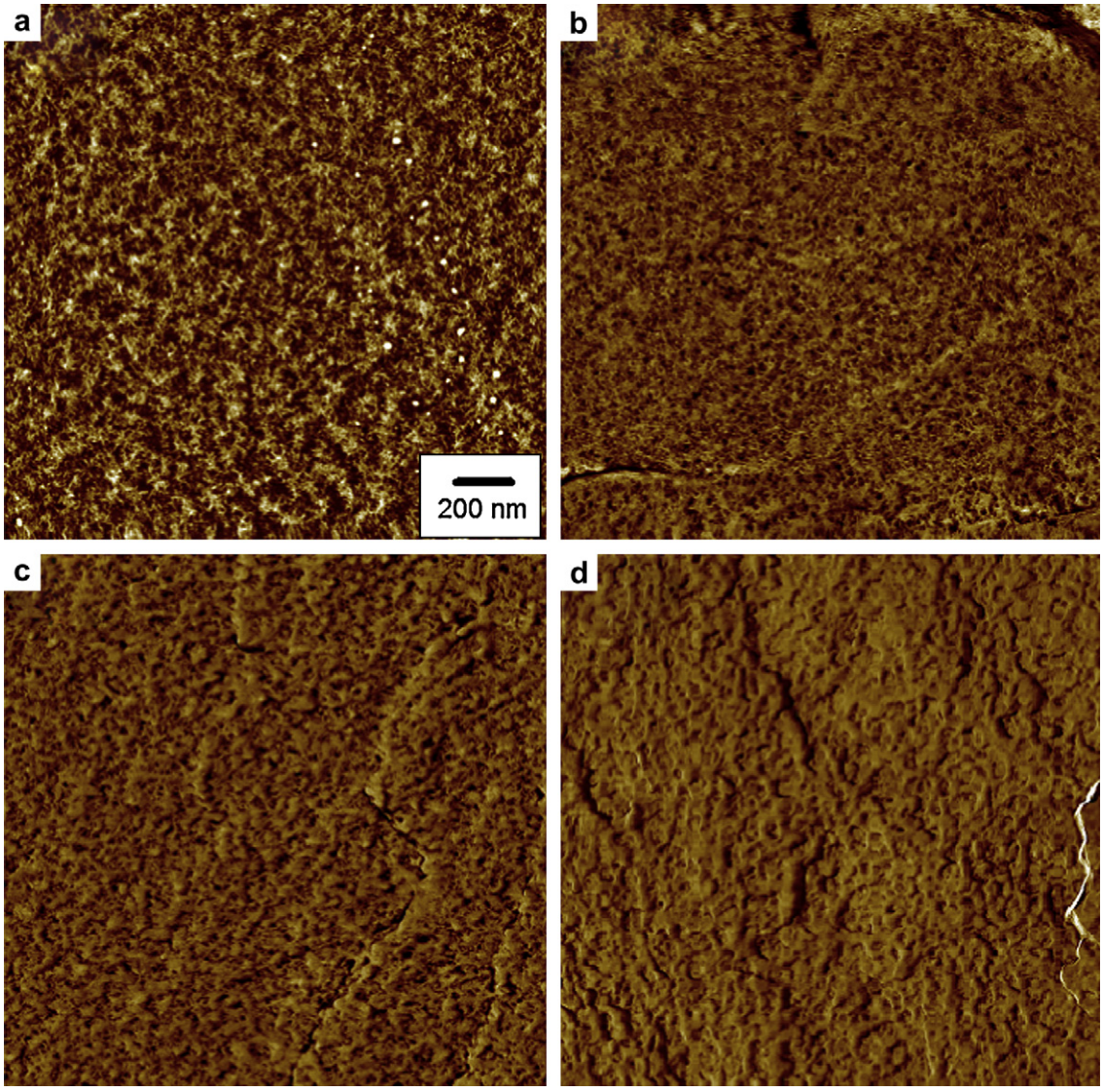

Fig. 8. Ambient, tapping mode AFM phase images of the fractured surfaces of segmented polyurethanes with (a) 70, (b) 60, (c) 50 and (d) 40% SSC.

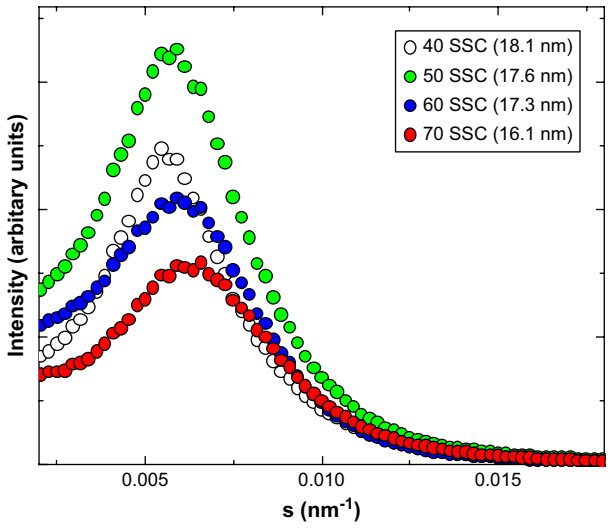

Fig. 9. SAXS profiles of the four segmented polyurethanes with varying SSCs (number in parenthesis in the legend indicates corresponding estimated interdomain spacings).

a more bicontinuous morphology of the hard and soft segments. The unexpected results show a small but a visible lowering of the soft segment glass transition with increasing hard segment content, which is clearer in the DMA data than in the DSC results, as shown in Table 2.

This indicates a higher mobility of the soft segments in the presence of larger hard domains, possibly as a result of a better microphase separation at higher hard segment concentrations.

The melting enthalpy of about 25 J/g for the polyurethane with 50% SSC is identical with that found in a polyurethane with 50% polypropylene oxide (PPO) soft segments and BD/MDI hard segments, suggesting the same degree of crystallinity [42]. However, melting enthalpy in the polyricinoleate-based polyurethane with 70% SSC was 8.4 J/g vs. 5 J/g for the PPO-based analogue. A clear melting point (170–200 °C) in the polyricinoleate polyurethane with 70% SSC displayed in Fig. 10 indicates a better phase separation.

DMA experiments were carried out in order to obtain further information on the microphase morphologies of the segmented polyurethanes with different soft segment concentrations. Fig. 11a and b displays the dependence of the storage modulus and loss modulus of the four segmented polyurethanes on temperature.

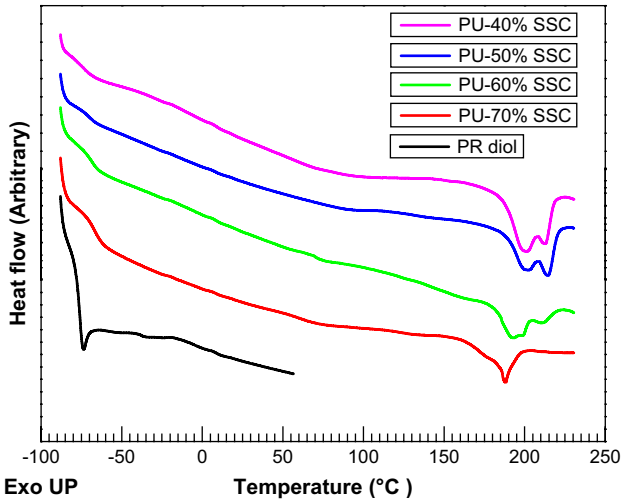

Fig. 10. DSC thermograms of polyurethanes at a heating rate of 10 °C/min.

Fig. 11 shows clearly that the rubbery plateau modulus of the segmented polyurethanes increased with the increase in the hard segment content which is believed to be due to the increased formation of a more continuous hard phase morphology. As expected, as the SSC increases, the modulus above the soft segment T_g systematically decreases due to less of a continuous hard segment phase with this change occurring within the SSC range of 50–70%. When the soft phase goes through its glass transition the modulus in the 70% SSC sample decreased about three orders in magnitude in contrast with the modulus of the 50% SSC sample where its more continuous hard phase could better bear the stress which maintained the modulus still at a high level, until the hard phase reached the glass transition somewhat below 100 °C. Above this temperature only crystalline regions of the hard phase acted more as a rigid physical crosslinks for the now relatively lower modulus soft segment phase. The sample with 60% SSC may have an intermediate morphology, possibly with both dispersed hard domains and some continuous structure. The high modulus up to *ca.* 100 °C for the two polyurethanes of 50 and 40% SSC is consistent with the DSC results shown in Fig. 10 regarding broad and quite weak glass transitions for the hard segments. In summary, with the SSC changing from 70 to 40%, the polyurethanes change from that of a soft rubber to a tougher rubber, and finally to what might be best described as a rubber-toughened plastic. This latter statement will be supported by their stress–strain behavior presented later.

3.7. Mechanical and rubbery properties of polyurethanes with different SSCs

Mechanical properties of segmented polyurethanes are closely related to their morphology and composition. The shape of stress–strain curves of samples with dispersed hard domains in the matrix of the soft phase is typical for elastomeric materials and can be sometimes roughly approximated by rubber elasticity theory [43]:

Table 2
Glass transitions of the soft and hard segments in polyricinoleate polyurethanes

SSC, %	T_{gss}		T_{ghs}	T_{ghs} (tan δ maximum)	Melting enthalpy, J/g
	By DSC	By DMA			
40	−71	−61	67 (E''_{max})	~115	25.6
50	−70	−59	–	96	24.7
60	−68	−56	70 (DSC)	93	13.5
70	−66	−56	65 (DSC)	–	8.43

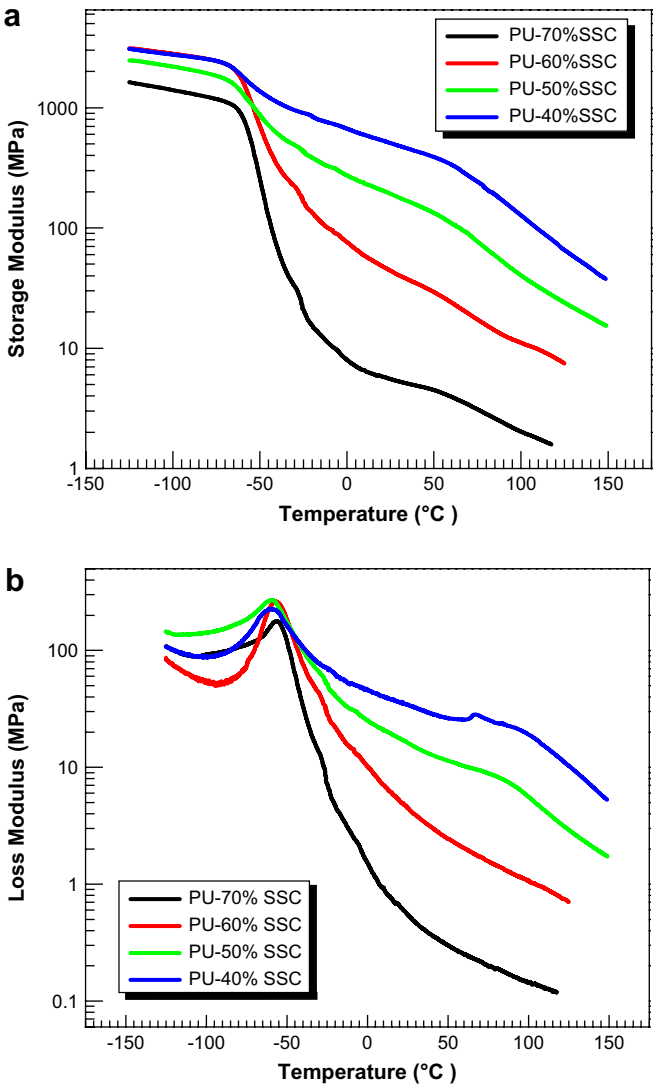

Fig. 11. (a) Storage and (b) loss moduli of polyurethanes (at 1 Hz and 3 °C/min).

$$\sigma = G\left(\lambda - l/\lambda^2\right) \quad (1)$$

Here, σ is the engineering stress in extension, G is shear modulus and λ is the extension ratio (l/l_o). Modulus is related in the present case to the variables of hard domain size, shape, connectivity and concentration. Fig. 12 shows the ambient stress–strain behavior of the four segmented polyurethanes, which were uniaxially deformed until failure. Results showed that while the polyurethanes with 40 and 50% SSC had higher modulus and an initially larger linear portion of the stress–strain curve relative to the polyurethanes with 60 and 70% SSC, the latter polyurethanes showed greater elastomeric behavior as exemplified by their higher recoverability (Fig. 13) and lower moduli. The polyurethane with 40% SSC also showed the presence of a distinct yield point, suggesting the existence of a relatively more continuous hard phase than the other polyurethanes studied. With decreasing soft segment concentration, both tensile modulus and the ultimate tensile strength of the segmented polyurethanes increased as expected. At the high SSC of 70%, the tensile strength is 2.8 MPa and elongation at break 67%; while these values increased to 18 MPa – 257%, and 26 MPa – 188% for the polyurethanes with SSC of 50 and 40%, respectively. It is recalled from the earlier discussion in Section 3.3 regarding the presence of the superstructures that these

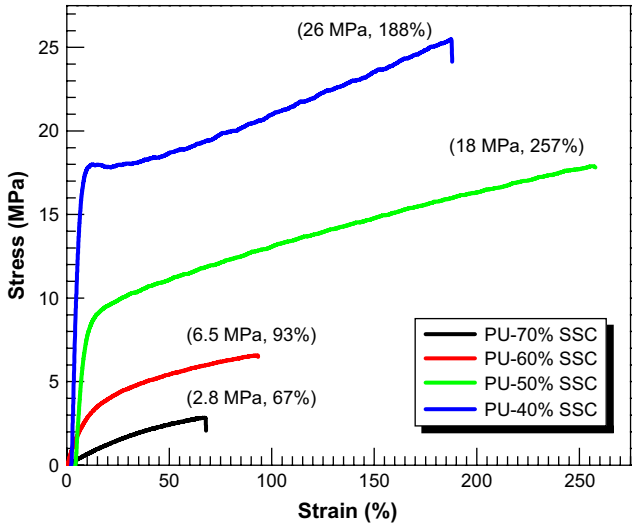

Fig. 12. Stress–strain behaviors of segmented polyurethanes.

entities promote some level of non-uniformity in texture due to their boundary impingement. As a result, such non-uniformities may promote points of stress concentration which could influence ultimate properties such as elongation at break and tensile strength. Thus, the reader is cautioned that these mechanical parameters reported here may be somewhat depressed in value relative to materials without such surface defects. The difference in the stress–strain behavior between the polyurethane with 70% SSC and 50% SSC was also significant, suggesting that the continuity of the hard and soft microphase behavior is changed, which is consistent with the results from DSC, DMA, and AFM.

$$\mathrm{MH\%} = [(\text{loading area}) - (\text{unloading area})/(\text{loading area})] \times 100 \quad (2)$$

Figs. 13 and 14 show the mechanical hysteresis behavior of the four segmented polyurethanes with various SSC%, when uniaxially deformed in a cyclic mode up to 50% strain under ambient conditions (50 mm/min strain rate). Results show that with increase in the SSC, the mechanical hysteresis (Eq. (2)), permanent set (described as the strain at zero stress in the unloading cycle) and the stress at 50% strain decreased systematically. Thus, the elastomeric properties of the polyurethanes increased, as expected, with increase in SSC%. The polyurethane system with 40% SSC again showed the presence of a distinct yield point in its loading cycle, strongly indicating the presence of longer range connectivity between the hard domains, which was absent in all the other polyurethanes characterized.

3.8. Thermal stability of segmented polyurethane elastomers

The thermal degradation of polyurethane is characterized by the decomposition of urethane bonds, the degradation of soft segments, and the evolution of the volatile components. Fig. 15a and b displays the TGA and DTG curves of the polyurethane elastomers.

The decomposition of polyricinoleate diol is characterized by a peak temperature at 377 °C. It is clearly shown that the decomposition below 420 °C of the segmented polyurethanes with the SSCs of 70, 60, 50, and 40%, was characterized by two peaks, one of which is almost the same as that observed for polyricinoleate decomposition, while the other is centered at 354 °C starting from about 220 °C. The 354 °C peak decreases with increasing SSC and decreasing urethane content and is believed to be from the thermal decomposition of urethane bonds, while the right hand side shoulder is clearly related to the decomposition of the polyricinoleate soft segment. Further decomposition in the region between 400 and 500 °C correlates well with the aromatic content in polyurethanes. These results indicate that polyricinoleate segmented polyurethanes are stable enough to be processed by injection molding and extrusion – particularly if conventional stabilizers are also added as is industrially practiced.

4. Summary

Based on the synthesis, characterization and structure–property data gathered on this novel series of segmented polyurethanes whose soft segments are based on ricinoleic acid moieties from castor oil and whose hard segments are derived from conventional MDI and BDO, the following summary comments are made:

(1) Success was achieved in the synthesis of these materials and their molecular characterization showed that control of hard/soft segment composition could be well controlled over a wide range.

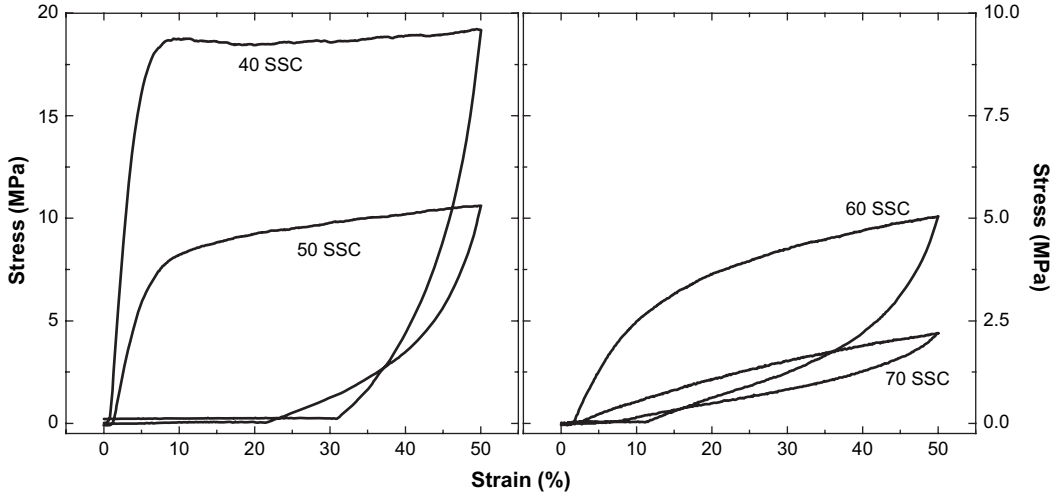

Fig. 13. Effect of variation of SSC on the cyclic deformation behavior of segmented polyurethanes (note that the *y*-axis scales in the two graphs are different).

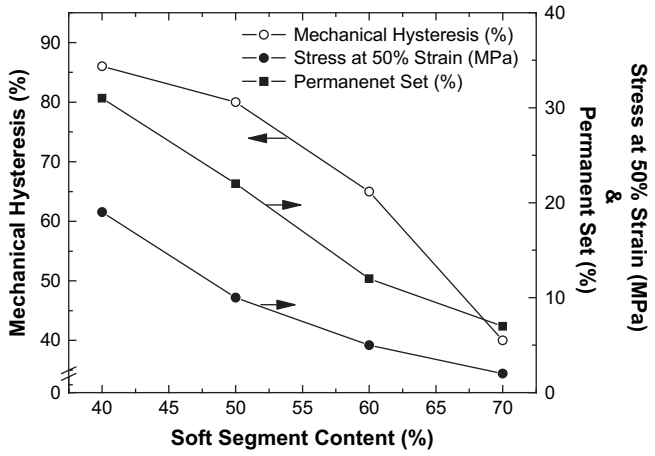

Fig. 14. Effect of SSC content on the viscoelastic properties of segmented polyurethanes.

(2) Molecular weight characterization showed that M_w of the four materials of varying hard segment content were reasonably high although it might be desirable to try and promote somewhat higher values for the 70% SSC system, since this might help improve the ultimate properties of this particular polymer.

(3) All four segmented systems displayed microphase separation by use of DSC, SAXS and AFM and surprisingly also showed evidence of a "spherulitic-like" superstructure at the 10 μm level by use of SEM – the latter superstructural elements are conjectured to arise from the nucleation and growth of hard segment crystalline regions. However, the presence of near transparency of all film materials suggested that these superstructural elements are lacking signs of optical anisotropy since no anisotropic scattering pattern was noted in any of the films by use of SALS. It would be of interest to probe the details of this interesting morphological texture in future work.

(4) The DMA profiles of the four materials were systematic and showed the expected increase in modulus above the soft segment T_g (−60 to −55 °C) as the hard segment content increased. The T_g of the hard segment was less distinct but it is suggested that this is somewhat near 100 °C.

(5) The ambient temperature stress–strain behavior in conjunction with limited hysteresis data clearly shows that these materials have the potential for a variety of structural applications depending on hard segment content. As expected, the lower hard segment content systems were of lower modulus and elastic/rubbery in behavior while the high hard segment content materials were stiffer and displayed less recovery following deformation. Interestingly, the presence of the six-carbon short "dangling" chain in each repeating unit of the soft segments does not limit the overall bulk properties.

(6) In view of the mechanical and thermal behaviors of these four materials, it is believed that these bio-based materials have the potential to be utilized in conventional TPU applications although it is expected that like conventional TPU systems, appropriate stabilizers would promote even further thermal stability during melt processing.

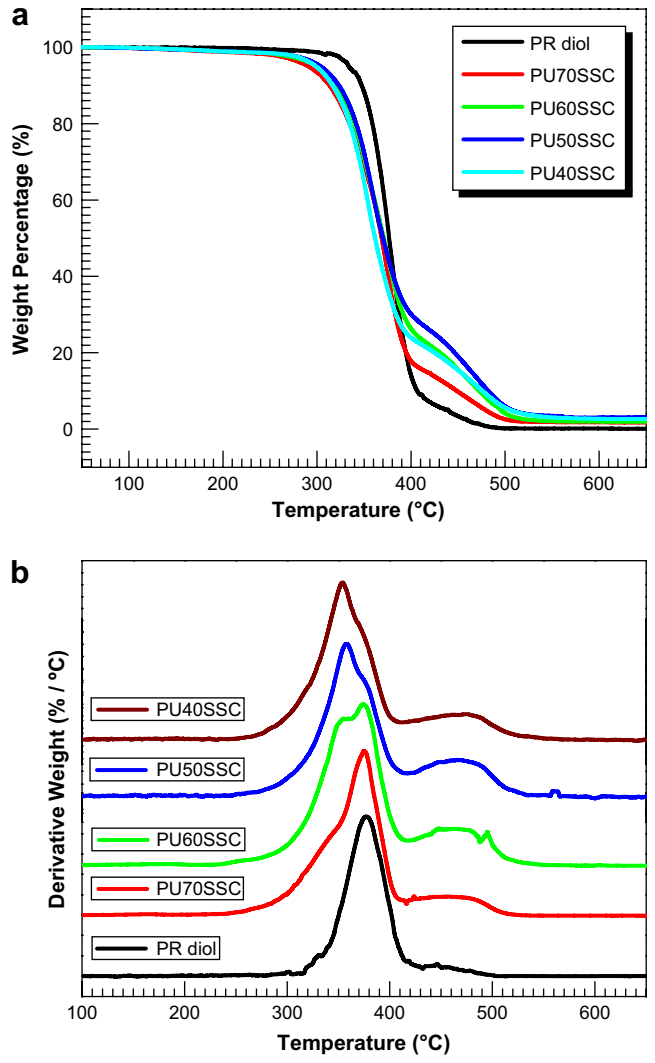

Fig. 15. (a) TGA and (b) DTG curves for polyricinoleate and segmented polyurethanes.

Acknowledgment

Two of the authors (GW and SD) would like to acknowledge the financial support of the United Soybean Board for the portion of the work carried out at Virginia Tech.

References

[1] Petrović ZS, Xu Y, Zhang W. Polymer Preprints 2007;48(2):852–3.
[2] Hepburn C. Polyurethane elastomers. 2nd ed. London: Elsevier; 1991.
[3] Oertel G. Polyurethane handbook. 2nd ed. Hanser; 1993.
[4] Harrell LL. Macromolecules 1969;2(6):607–12.
[5] Petrović ZS, Ferguson J. Progress in Polymer Science 1991;16:695–836.
[6] Li C, Goodman SL, Albrecht RM, Cooper SL. Macromolecules 1988;21(8):2367–75.
[7] Petrović ZS, Javni I. Journal of Polymer Science, Part B: Polymer Physics 1989;27(3):545–60.
[8] Petrović ZS, Budinski-Simendić J. Rubber Chemistry and Technology 1985;58:685–700.
[9] Wilkes GL, Samuels SL. Rheo optical studies of block and segmented copolymers – a review. In: Burke J, Weiss V, editors. Block and graft copolymers. Syracuse: Syracuse University Press; 1973.
[10] Samuels SL, Wilkes GL. Journal of Polymer Science Polymer Letter Edition 1971;9:761–6.
[11] Samuels SL, Wilkes GL. Journal of Polymer Science Polymer Physics Edition 1973;11(4):807–11.
[12] Aneja A, Wilkes GL. Polymer 2003;44(23):7221–8.
[13] Gander K. Journal of the American Oil Chemists' Society 1984;61(2):268–71.
[14] Baumann H, Bühler M, Fochem H, Hirsinger F, Zoebelein H, Jürgen Falbe. Angewandte Chemie International Edition in English 1988;27(1):41–62.
[15] Derksen JTP, Cuperus FP, Kolster P. Industrial Crops and Products 1995;3(4):225–36.
[16] Heidbreder A, Höfer R, Grützmacher R, Westfechtel A, Blewett CW. Fett – Lipid 1999;101(11):418–24.
[17] Hill K. Pure and Applied Chemistry 2000;72(7):1255–64.
[18] Nayak PL. Polymer Reviews 2000;40(1):1–21.

[19] Biermann U, Friedt W, Lang S, Lühs W, Machmüller G, Metzger JO, et al. Angewandte Chemie International Edition 2000;39(13):2206–24.
[20] Warwel S, Bruse F, Demes C, Kunz M, Klaas MRg. Chemosphere 2001;43(1):39–48.
[21] Guner FS, Yagci Y, Erciyes AT. Progress in Polymer Science 2006;31(7):633–70.
[22] Sharma V, Kundu PP. Progress in Polymer Science 2006;31(11):983–1008.
[23] Kohlhase W, Pryde E, Cowan J. Journal of the American Oil Chemists' Society 1970;47(5):183–8.
[24] Petrović ZS. Polymer Reviews 2008;48(1):109–55.
[25] Guo A, Javni I, Petrović ZS. Journal of Applied Polymer Science 2000;77: 467–73.
[26] Guo A, Zhang W, Petrović Z. Journal of Materials Science 2006;41(15): 4914–20.
[27] Guo A, Demydov D, Zhang W, Petrović ZS. Journal of Polymers and the Environment 2002;10(1):49–52.
[28] Zlatanić A, Petrović ZS, Dušek K. Biomacromolecules 2002;3(5):1048–56.
[29] Petrović ZS, Zhang W, Javni I. Biomacromolecules 2005;6(2):713–9.
[30] Uchida Y, Yoshida Y, Kaneda T, Moriya T, Kumazawa T. Elastomer and process for production thereof. US: Mitsui Toatsu Chemicals, Inc.; 1994.
[31] Petrović ZS, Cvetković I, Hong D, Wan X, Zhang W, Abraham T, et al. Journal of Applied Polymer Science 2008;108(2):1184–90.
[32] Aneja A, Wilkes GL. Polymer 2004;45:927–35.
[33] Holden G, Lagge NR, Quirk R, Schroeder HE. Thermoplastic elastomers. 2nd ed. New York: Hanser Publishers; 1996.
[34] Noshay A, McGrath JE. Block copolymers: overview and critical survey. New York: Academic Press; 1977.
[35] Seymour RW, Cooper SL. Macromolecules 1973;6(1):48–53.
[36] Leung LM, Koberstein JT. Macromolecules 1986;19(3):706–13.
[37] Koberstein JT, Russell TP. Macromolecules 1986;19(3):714–20.
[38] Koberstein JT, Galambos AF. Macromolecules 1992;25(21):5618–24.
[39] Chen TK, Shieh TS, Chui JY. Macromolecules 1998;31(4):1312–20.
[40] Saiani A, Novak A, Rodier L, Eeckhaut G, Leenslag J-W, Higgins JS. Macromolecules 2007;40(20):7252–62.
[41] Ebata H, Toshima K, Matsumura S. Macromolecular Bioscience 2007;7(6):798–803.
[42] Petrović ZS, Javni I, Divjaković V. Journal of Polymer Science, Part B: Polymer Physics 1998;36:221–35.
[43] Treloar LRG. The physics of rubber elasticity. Oxford: Clarendon Press; 1958.